Guest-dependent negative thermal expansion in a lanthanide-based metal–organic framework

Andrzej Gładysiak,[a] Seyed Mohamad Moosavi,[a] Lev Sarkisov,[b] Berend Smit[a] and Kyriakos C. Stylianou[a]*

[a]*Laboratory of Molecular Simulation (LSMO), Institut des Sciences et Ingénierie Chimiques (ISIC), École Polytechnique Fédérale de Lausanne (EPFL) Valais, Rue de l'Industrie 17, 1951 Sion, Switzerland.*

[b]*Institute for Materials and Processes, School of Engineering, The University of Edinburgh, EH9 3JL, UK*

E-mail: kyriakos.stylianou@epfl.ch

Supporting information

Table S1 A summary of properties of various NTE-exhibiting materials. Coefficients of thermal expansion are expressed in MK^{-1} and refer to the principal axes X_1, X_2, and X_3 unless otherwise stated. Asterisk refers to materials exhibiting PTE, but included here for comparison. TVM = transverse vibrational modes, HG = host–guest interactions, H = hinging, MPR = molecular packing rearrangement, SC = spin-crossover.

	α_1	α_2	α_3	Space group	Ref.	Temp. range	Mechanism	Notes
calcite	−3.7	.	+25.6	$R\bar{3}c$	1	303−363 K	(an early report)	
graphite	−1.5	.	+28.3	$P6_3/mmc$	2	273−423 K	(an early report)	
β-USi_2	+57	.	−26	$P6/mmm$	3	293−478 K	(an early report)	
ZrW_2O_8	−9.1	.	.	$P2_13$(lt), $Pa\bar{3}$ (ht)	4	0.3−1050 K	TVM	
MOF-5	−13.1(1)	.	.	$Fm\bar{3}m$	5	80−500 K	TVM	
$Zn(CN)_2$	−16.9(2)	.	.	$Pn\bar{3}m$	6	25−375 K	TVM	
$Zn_{0.80}Cd_{0.20}(CN)_2$	−17.8(2)	.	.	$Pn\bar{3}m$	6	100−375 K	TVM	
$Zn_{0.64}Cd_{0.36}(CN)_2$	−19.5(3)	.	.	$Pn\bar{3}m$	6	100−375 K	TVM	
$Cd(CN)_2$	−20.4(4)	.	.	$Pn\bar{3}m$	6	150−375 K	TVM	
HKUST-1 = $Cu_3(btc)_2$	−4.9(1)	.	.	$Fm\bar{3}m$	7	100−300K	TVM	

$Cu_3(btb)_2$	−13	.	.	$Im\bar{3}$	[8]	3−400 K	TVM	
$Sc_2(WO_4)_3$	−2.2	.	.	*Pnca*	[9]	10−1073 K	TVM	average α given
MIL-68(In)	−5.6	−2.7	−4	*Cmcm*	[10]	125−600 K	TVM	
ScF_3	−14	.	.	$Pm\bar{3}m$	[11]	60−110 K	TVM	
$Li_{0.06}(Sc_{0.90}Fe_{0.10})F_3$*	+1.03	.	.	$Pm\bar{3}m$	[12]	150−425 K	TVM + HG	
$Li_{0.04}(Sc_{0.94}Fe_{0.06})F_3$	−0.75	.	.	$Pm\bar{3}m$	[12]	150−425 K	TVM + HG	
$Li_{0.06}(Sc_{0.97}Fe_{0.03})F_3$	−2.59	.	.	$Pm\bar{3}m$	[12]	150−425 K	TVM + HG	
ScF_3	−7.40	.	.	$Pm\bar{3}m$	[12]	150−425 K	TVM + HG	
$ZrMo_2O_8$	−5.9(2)	.	.	$Pa\bar{3}$	[13]	12−500 K	TVM	
$Zr_{0.4}Sn_{0.6}Mo_2O_8$	−6(20)	.	.	$Pa\bar{3}$	[13]	12−600 K	TVM	
$SnMo_2O_8$*	+7.9(2)	.	.	$Pa\bar{3}$	[13]	10−500 K	TVM	
$LiBeBO_3$	−3.31(13)	−1.76(8)	+7.6(7)	$P\bar{1}$	[14]	73−193 K	TVM	
$PbTiO_3$	+29	.	−71	*P*4*mm*	[15]	473−673 K	TVM	
$PbTiO_3$	+38	.	−108	*P*4*mm*	[15]	673−753 K	TVM	
$LiAlSi_4O_{10}$	−3	+2	−10	*P*2/*a*	[16]	100−110 K	TVM	
$LiAlSi_4O_{10}$	+3	+14	−3	*P*2/*a*	[16]	500−600 K	TVM	
$Cd(im)_2$	+92.6(16)	−22.5(5)	+19.6(7)	*Pbca*	[17]	100−300 K	TVM (rotations of tetrahedra)	
V_2OPO_4-II	−8	.	+9	$I4_1/amd$	[18]	610−750 K	TVM	
$ZnPt(CN)_6{\cdot}2H_2O$*	+1.82(15)	.	.	$Fm\bar{3}m$	[19]	100−250 K	TVM + HG	
$ZnPt(CN)_6$	−3.38(9)	.	.	$Fm\bar{3}m$	[19]	375−25 K	TVM	
$CdPt(CN)_6{\cdot}2H_2O$	−7.31(5)	.	.	$Fm\bar{3}m$	[19]	100−250 K	TVM + HG	
$CdPt(CN)_6$	−6.69(5)	.	.	$Fm\bar{3}m$	[19]	375−25 K	TVM	
$Cd(CN)_2{\cdot}CCl_4$*	+10.0(2)	.	.	$Fd\bar{3}m$	[20]	100−240 K	TVM + HG	
$Cd(CN)_2{\cdot}0.75CCl_4$	−5.7(3)	.	.	$Fd\bar{3}m$	[20]	200−375 K	TVM + HG	
$Cd(CN)_2{\cdot}0.64CCl_4$	−16.9(3)	.	.	$Fd\bar{3}m$	[20]	240−375 K	TVM + HG	
$Cd(CN)_2$	−33.5(5)	.	.	$Fd\bar{3}m$	[20]	170−375 K	TVM	
$YFe(CN)_6$	−11.92	.	−9.94	$P6_3/mmc$	[21]	300−525 K	TVM	
$YFe(CN)_6{\cdot}4H_2O$	−7.49	+22.08	+13.09	*Cmcm*	[21]	125−300 K	TVM + HG	
$KYFe(CN)_6{\cdot}3H_2O$	+25.67	+12.27	+4.71	*Pbnm*	[21]	125−300 K	TVM + HG	
$KYFe(CN)_6$	+11.84	.	−3.43	$P\bar{3}1c$	[21]	300−525 K	TVM	
$LaCo(CN)_6$	−16.58(5)	.	−10.68(7)	$P6_3/mmc$	[22]	100−500 K	TVM	α along *x*, *y*, *z*
$SmCo(CN)_6$	−12.53(14)	.	−12.31(9)	$P6_3/mmc$	[22]	100−500 K	TVM	
$HoCo(CN)_6$	−10.06(5)	.	−10.05(7)	$P6_3/mmc$	[22]	100−500 K	TVM	
$LuCo(CN)_6$	−9.56(6)	.	−8.03(7)	$P6_3/mmc$	[22]	100−500 K	TVM	
$YCo(CN)_6$	−10.67(4)	.	−10.25(6)	$P6_3/mmc$	[22]	100−500 K	TVM	
$Ni(CN)_2$	−6.5(1)	.	+61.8(3)	$P4_2/mmc$	[23]	28−300 K	TVM	
$AlPO_4$-17 (ERI)	−15.3	.	−4.52	$P6_3/m$	[24]	18−300 K	TVM	
ITQ-1 zeolite	−4.23	.	−3.21	*P*6/*mmm*	[25]	323−773 K	TVM	
ITQ-3 zeolite	−0.29	−2.06	−10.1	*Cmcm*	[25]	323−823 K	TVM	
SSZ-23 zeolite	−6.09	−3.21	−0.73	$P2_1/n$	[25]	323−773 K	TVM	
ITQ-4 zeolite	−11.5	−7.47	+7.19	*I*2/*m*	[26]	95−510 K	TVM	
CHA zeolite	−8.24	.	−13.3	$R\bar{3}m$	[26]	293−873 K	TVM	
ITQ-7 zeolite	−2.28	.	−1.05	$P4_2/mmc$	[27]	473−873 K	TVM	
ITQ-9 zeolite	−5.58	−2.37	−2.19	$I\bar{1}$	[27]	293−873 K	TVM	

MAPO-17 zeolite	−9.16	.	+4.66	$P6_3/m$	[27]	323−773 K	TVM	
FER zeolite	+8.1	−2.8	+16.1	$Pnnm$	[28]	150−400 K	TVM	
FER zeolite	−6.7	−7.1	−10.6	$Immm$	[28]	420−560 K	TVM	
FAU zeolite	−4.0	.	.	$Fd\bar{3}m$	[29]	298−923 K	TVM	
FAU zeolite*	+10.0	.	.	$Fd\bar{3}m$	[29]	923−1123 K	TVM	
ITQ-29 zeolite	−5.55	.	.	$Pm\bar{3}m$	[30]	293−1173 K	TVM	
USY zeolite	−30	.	.	$Fd\bar{3}m$	[31]	773−1073 K	TVM	
LaY zeolite	−7.5	.	.	$Fd\bar{3}m$	[31]	773−1073 K		
$(CD_3)_2CO{\cdot}Br_2$	−39.6	−18.2	+157.6	$C2/c$	[32]	14−37 K	TVM + contribution from H	
$(CD_3)_2CO{\cdot}Br_2$*	+42.4	+67.3	+169.3	$C2/c$	[32]	47−200 K	TVM + contribution from H	
$Ag_3[Co(CN)_6]$	−126(4)	+144(9)	.	$P\bar{3}1m$	[33]	16−500 K	H + contribution from TVM	
Ag(mim)	+130(2)	+44(3)	−24.5(8)	$P2_1/n$	[34]	20−300 K	H + contribution from TVM	
$[NH_2NH_3][Tm(HCOO)_4]$	+100	+100	−120	$Pca2_1$	[35]	100−180 K	H + contribution from TVM	
$[NH_2NH_3][Tm(HCOO)_4]$	+50	+10	+10	$Pca2_1$	[35]	180−375 K	H + contribution from TVM	
$[Fe(dpp)_2(NCS)_2]{\cdot}$py-HS	−84	+221	+19.4	$P2/n$	[36]	150−275 K	H	α along x, y, z
$KMn[Ag(CN)_2]_3$	+61(2)	.	−60(3)	$P312$	[37]	100−300 K	H	
$Zn(ISN)_2$	−10.9(5)	.	+64(3)	$P6_2$	[38]	10−300 K	H	α along x, y, z
$InD(BDC)_2$	+60(3)	.	−35(2)	$P6_422$	[38]	10−300 K	H	α along x, y, z
$Li(4\text{-pyc})(H_2O)_{0.5}{\cdot}0.5MeOH$	−42(2)	+3(2)	+206(4)	$C2/c$	[39]	100−260 K	H	
Ag(tcm)	−48(3)	+200(2)	−54.0(4)	$Ima2$	[40]	100−250 K	H	
$[NH_2CHNH_2][Er(HCOO)_4]$	+11.7(11)	−7.1(3)	+10.0(7)	$C222_1$	[41]	60−300 K	H	
FJI-H11-Me	−37.8(2)	.	+653.2(5)	$R\bar{3}m$	[42]	100−300 K	H	
FJI-H11-Et	−33.2(3)	.	+489.4(10)	$R\bar{3}m$	[42]	100−300 K	H	
FJI-H11-iPr	−24.6(2)	.	+403.7(4)	$R\bar{3}m$	[42]	100−300 K	H	
$Zn(eim)_2$	+30	+30	−21	$P3_121$	[43]	123−473 K	H	
$Cd(eim)_2$	+66	+66	−55	$P3_121$	[43]	123−473 K	H	
$[Zn_2(fu\text{-}L^1)_2dabco]$-np	−94.3	+373	+5.20	$P2_1/m$	[44]	303−463 K	H	α along x, y, z
$[Zn_2(fu\text{-}L^2)_2dabco]$-np	−129	+402	+16.1	$C2/m$	[44]	303 393 K	H	
HMOF-1	+177	−21	+8	$Pnnm$	[45]	100−297 K	H	
$CD_3OD{\cdot}D_2O$	−61(4)	+462(4)	+93(4)	$Cmc2_1$	[46]	4.2−160 K	H	
β-2,4-dinitroanisole	−31(6)	−15(7)	+262(20)	$P2_1/n$	[47]	100−261 K	H	
$[Cd(HBTC)(BPP)]{\cdot}1.5DMF{\cdot}2H_2O$	−43.4(7)	+2(1)	+133(2)	$P\bar{1}$	[48]	100-260 K	H	
MCF-82	+61(1)	+482(12)	−218(3)	$P2_1/c$	[49]	112−300 K	H	
MCF-82·DMF	+171(4)	+60(3)	−56(2)	$P2_1/c$	[49]	112−300 K	H + HG	
MCF-82·DMA	+85(1)	+103(4)	−51(3)	$P2_1/c$	[49]	112−300 K	H + HG	
$Zn(niba)_2(OH)_2$	−26(5)	.	+137(5)	$I\bar{4}$	[50]	100−295 K	H	
$Zn(niba)_2(OH)_2{\cdot}MeOH$	−41(3)	.	+166(4)	$I\bar{4}$	[50]	100−295 K	H + HG	
$Zn(niba)_2(OH)_2{\cdot}EtOH$	−17(5)	.	+144(5)	$I\bar{4}$	[50]	100−295 K	H + HG	
$Zn(niba)_2(OH)_2{\cdot}n$-PrOH	−38(4)	.	+138(4)	$I\bar{4}$	[50]	100−295 K	H + HG	
$Zn(niba)_2(OH)_2{\cdot}i$-PrOH*	+23(6)	.	+76(6)	$I\bar{4}$	[50]	100−295 K	H + HG	
$[Ag(en)]NO_3$-I	−89.7(15)	+37.9(12)	+149.2(12)	$C2/c$	[51]	120−360 K	H + HG	
MCF-34	+2(1)	+244(1)	−107(1)	$I2/a$	[52]	127−673 K	H + HG	
MCF-34-LT.DMF	+16(2)	+152(3)	−56(5)	$P2_1/c$	[52]	127−208 K	H + HG	
MCF-34-HT.DMF	+36(4)	+237(6)	−116(5)	$I2/a$	[52]	133−299 K	H + HG	

(*S*,*S*)-octa-3,5-diyn-2,7-diol-HT	+533(56)	−72(13)	−190(25)	$P2_12_12_1$	[53]	225−330 K	MPR
pyridine-IBr	+176	−38	+88	$P2_1/c$	[54]	110−298 K	MPR
pyridine-ICl	+147	−7	+57	$P2_1/c$	[54]	110−298 K	MPR
4,4′-methylenebis(2,6-dimethylaniline)-II	−174(8)	+174(3)	+229(3)	$C2/c$	[55]	148−298 K	MPR
(phenylazophenyl)palladium hexafluoroacetylacetonate-α	+240.4(3)	+39.4(4)	−79.9(2)	$P\bar{1}$	[56]	223−348 K	MPR
1,1,4,4-tetrakis(4-hydroxyphenyl)cyclohexane	−8(2)	+27(2)	+71(2)	$P\bar{1}$	[57]	118−298 K	MPR
1,1,4,4-tetrakis(4-hydroxyphenyl)cyclohexane·phenol	−100(8)	+38(2)	+276(15)	$P\bar{1}$	[57]	105−298 K	MPR
1,1,4,4-tetrakis(4-hydroxyphenyl)cyclohexane·*m*-cresol*	+29(3)	+53(2)	+68(2)	$P\bar{1}$	[57]	120−298 K	MPR
1,1,4,4-tetrakis(4-hydroxyphenyl)cyclohexane·*p*-cresol	−50(2)	+47(1)	+176(4)	$P\bar{1}$	[57]	115−298 K	MPR
1,1,4,4-tetrakis(4-hydroxyphenyl)-cyclohexane·*o*-cresol-1D	−23(4)	−3(8)	+148(5)	$P\bar{1}$	[57]	120−298 K	MPR
1,1,4,4-tetrakis(4-hydroxyphenyl)-cyclohexane·*o*-cresol-2D*	+18(3)	+40(1)	+69(1)	$P2_1/n$	[57]	115−298 K	MPR
18-crown-6·2CH_3NO_2	−129(15)	+144(14)	+282(16)	$P2_1/n$	[58]	90−273 K	MPR + HG
18-crown-6·2CH_3I*	+17	+85	+131	$P2_1/n$	[58]	90−273 K	MPR + HG
Edimim[Cl]	−12.8(6)	+7.03(2)	+187(2)	$P2_1/a$	[59]	100−350 K	MPR + HG
Edimim[Br]	−40(2)	−64.4(3)	+301(3)	$P2_1/a$	[59]	100−350 K	MPR + HG
$[Fe_{0.84}Ni_{0.16}(bpac)(Au(CN)_2)_2]$·2EtOH	−3200	+5200	+1500	*Cmma*	[60]	216 K	SC
$[Fe_{0.68}Ni_{0.32}(bpac)(Au(CN)_2)_2]$·2EtOH	−540	+850	+310	*Cmma*	[60]	216 K	SC
$[Fe_{0.57}Ni_{0.43}(bpac)(Au(CN)_2)_2]$·2EtOH	−550	+970	+390	*Cmma*	[60]	215 K	SC
$[Fe_{0.35}Ni_{0.65}(bpac)(Au(CN)_2)_2]$·2EtOH	−270	+350	+150	*Cmma*	[60]	218 K	SC

Table S2 Selected crystallographic and structure refinement data for **SION-2** in the 100–380 K temperature range on heating.

Temperature/K	100	120	140	160
Empirical formula	$C_{21}H_{27}N_3O_{12}Tb$	$C_{21}H_{27}N_3O_{12}Tb$	$C_{21}H_{27}N_3O_{12}Tb$	$C_{21}H_{27}N_3O_{12}Tb$
Formula weight	672.37	672.37	672.37	672.37
Space group	$P\bar{1}$	$P\bar{1}$	$P\bar{1}$	$P\bar{1}$
a/Å	10.5096(6)	10.5156(6)	10.4937(6)	10.5194(6)
b/Å	10.9768(4)	10.9858(4)	10.9559(4)	10.9889(4)
c/Å	12.5019(6)	12.5290(6)	12.5321(6)	12.5734(6)
α/°	104.759(4)	104.707(4)	104.652(4)	104.589(4)
β/°	107.340(5)	107.578(5)	107.923(4)	108.172(5)
γ/°	97.380(4)	97.265(4)	97.114(4)	96.992(4)
Volume/Å^3	1298.23(12)	1301.80(12)	1294.06(11)	1304.34(12)
Z	2	2	2	2
ρ_{calc} g/cm^3	1.72	1.715	1.726	1.712
μ/mm^{-1}	2.79	2.782	2.798	2.776
F(000)	670	670	670	670
Wavelength/Å	0.71420	0.71420	0.71420	0.71420
2Θ range for data collection/°	3.954 to 56.862	3.948 to 56.852	3.958 to 56.864	3.944 to 56.854
Index ranges	$-13 \le h \le 13$, $-14 \le k \le 14$, $-13 \le l \le 13$	$-13 \le h \le 13$, $-14 \le k \le 14$, $-13 \le l \le 13$	$-13 \le h \le 13$, $-14 \le k \le 14$, $-13 \le l \le 13$	$-13 \le h \le 13$, $-14 \le k \le 14$, $-13 \le l \le 13$
Reflections collected	8177	8235	8291	8395
R_{int}, R_{sigma}	$R_{int} = 0.0174$, $R_{sigma} = 0.0261$	$R_{int} = 0.0166$, $R_{sigma} = 0.0250$	$R_{int} = 0.0162$, $R_{sigma} = 0.0244$	$R_{int} = 0.0166$, $R_{sigma} = 0.0245$
Data/restraints/parameters	4196/75/383	4216/73/383	4244/58/383	4303/58/383
Goodness of fit on F^2	1.1	1.11	1.07	1.051
Final R indexes [I≥2σ(I)]	$R_1 = 0.0330$, $wR_2 = 0.0938$	$R_1 = 0.0309$, $wR_2 = 0.0886$	$R_1 = 0.0295$, $wR_2 = 0.0857$	$R_1 = 0.0276$, $wR_2 = 0.0785$
Final R indexes [all data]	$R_1 = 0.0349$, $wR_2 = 0.0948$	$R_1 = 0.0327$, $wR_2 = 0.0896$	$R_1 = 0.0311$, $wR_2 = 0.0866$	$R_1 = 0.0291$, $wR_2 = 0.0792$
Largest diff. peak/hole / e Å^{-3}	1.91/–1.53	1.52/–1.40	1.29/–1.45	1.03/–1.23
CCDC	1871302	1871305	1871308	1871303

Temperature/K	180	200	220	240
Empirical formula	$C_{21}H_{27}N_3O_{12}Tb$	$C_{21}H_{27}N_3O_{12}Tb$	$C_{21}H_{27}N_3O_{12}Tb$	$C_{21}H_{27}N_3O_{12}Tb$
Formula weight	672.37	672.37	672.37	672.37
Space group	$P\bar{1}$	$P\bar{1}$	$P\bar{1}$	$P\bar{1}$
a/Å	10.5256(6)	10.5213(5)	10.5190(6)	10.5121(6)
b/Å	10.9947(5)	10.9954(5)	10.9933(5)	10.9835(5)
c/Å	12.6032(6)	12.6323(5)	12.6565(5)	12.6782(5)
α/°	104.523(4)	104.438(4)	104.317(4)	104.175(4)
β/°	108.540(5)	108.872(4)	109.262(4)	109.639(4)
γ/°	96.829(4)	96.664(4)	96.536(4)	96.452(4)
Volume/Å^3	1306.91(12)	1307.93(11)	1307.83(12)	1305.96(12)
Z	2	2	2	2
ρ_{calc} g/cm^3	1.709	1.707	1.707	1.71
μ/mm^{-1}	2.771	2.769	2.769	2.773
F(000)	670	670	670	670
Wavelength/Å	0.71420	0.71420	0.71420	0.71420
2Θ range for data collection/°	3.938 to 56.866	3.936 to 56.85	3.934 to 56.862	3.934 to 56.856
Index ranges	$-13 \le h \le 13$, $-14 \le k \le 14$, $-13 \le l \le 13$	$-13 \le h \le 13$, $-14 \le k \le 14$, $-13 \le l \le 13$	$-13 \le h \le 13$, $-14 \le k \le 14$, $-13 \le l \le 13$	$-13 \le h \le 13$, $-14 \le k \le 14$, $-13 \le l \le 13$
Reflections collected	8523	8611	8658	8597
R_{int}, R_{sigma}	$R_{int} = 0.0175$, $R_{sigma} = 0.0261$	$R_{int} = 0.0172$, $R_{sigma} = 0.0249$	$R_{int} = 0.0176$, $R_{sigma} = 0.0259$	$R_{int} = 0.0162$, $R_{sigma} = 0.0231$
Data/restraints/parameters	4360/58/383	4413/58/383	4433/58/383	4401/58/383
Goodness of fit on F^2	0.999	1.074	1.048	1.07
Final R indexes [I≥2σ(I)]	$R_1 = 0.0430$, $wR_2 = 0.1147$	$R_1 = 0.0288$, $wR_2 = 0.0784$	$R_1 = 0.0313$, $wR_2 = 0.0836$	$R_1 = 0.0267$, $wR_2 = 0.0735$
Final R indexes [all data]	$R_1 = 0.0444$, $wR_2 = 0.1160$	$R_1 = 0.0300$, $wR_2 = 0.0792$	$R_1 = 0.0325$, $wR_2 = 0.0846$	$R_1 = 0.0280$, $wR_2 = 0.0743$
Largest diff. peak/hole / e Å^{-3}	2.07/–3.81	1.16/–1.45	1.69/–1.43	1.43/–1.39
CCDC	1871306	1871304	1871311	1871307

Temperature/K	260	280	300	320
Empirical formula	$C_{21}H_{27}N_3O_{12}Tb$	$C_{21}H_{27}N_3O_{12}Tb$	$C_{21}H_{27}N_3O_{12}Tb$	$C_{21}H_{27}N_3O_{12}Tb$
Formula weight	672.37	672.37	672.37	672.37
Space group	$P\bar{1}$	$P\bar{1}$	$P\bar{1}$	$P\bar{1}$
a/Å	10.5371(6)	10.5333(6)	10.5445(7)	10.5861(8)
b/Å	11.0161(5)	11.0035(5)	11.0141(6)	11.0497(6)
c/Å	12.7345(5)	12.7511(5)	12.7860(8)	12.8741(10)
α/°	104.005(5)	103.784(5)	103.484(5)	103.021(6)
β/°	109.918(4)	110.271(4)	110.657(6)	111.135(7)
γ/°	96.448(4)	96.437(4)	96.519(5)	96.698(5)
Volume/Å^3	1317.37(12)	1315.34(12)	1319.52(15)	1335.67(18)
Z	2	2	2	2
ρ_{calc} g/cm^3	1.695	1.698	1.692	1.672
μ/mm^{-1}	2.749	2.753	2.745	2.711
F(000)	670	670	670	670
Wavelength/Å	0.71420	0.71420	0.71420	0.71420
2Θ range for data collection/°	3.92 to 56.866	3.92 to 56.862	3.914 to 56.858	3.896 to 56.864
Index ranges	$-13 \le h \le 13$, $-14 \le k \le 14$, $-13 \le l \le 13$	$-13 \le h \le 13$, $-14 \le k \le 14$, $-13 \le l \le 13$	$-13 \le h \le 13$, $-14 \le k \le 14$, $-13 \le l \le 13$	$-13 \le h \le 13$, $-14 \le k \le 14$, $-13 \le l \le 13$
Reflections collected	8661	8650	8650	8727
R_{int}, R_{sigma}	$R_{int} = 0.0155$, $R_{sigma} = 0.0229$	$R_{int} = 0.0169$, $R_{sigma} = 0.0251$	$R_{int} = 0.0185$, $R_{sigma} = 0.0271$	$R_{int} = 0.0202$, $R_{sigma} = 0.0304$
Data/restraints/parameters	4426/115/374	4430/127/374	4443/129/374	4471/135/374
Goodness of fit on F^2	1.081	1.076	1.084	1.074
Final R indexes [I≥2σ(I)]	$R_1 = 0.0249$, $wR_2 = 0.0700$	$R_1 = 0.0259$, $wR_2 = 0.0693$	$R_1 = 0.0285$, $wR_2 = 0.0774$	$R_1 = 0.0324$, $wR_2 = 0.0922$
Final R indexes [all data]	$R_1 = 0.0262$, $wR_2 = 0.0706$	$R_1 = 0.0272$, $wR_2 = 0.0698$	$R_1 = 0.0303$, $wR_2 = 0.0784$	$R_1 = 0.0346$, $wR_2 = 0.0937$
Largest diff. peak/hole / e Å^{-3}	1.02/–1.14	1.16/–1.20	1.20/–1.16	1.56/–1.21
CCDC	1871309	1871310	1871313	1871312

Temperature/K	340	360	380
Empirical formula	$C_{21}H_{27}N_3O_{12}Tb$	$C_{19.01}H_{22.36}N_{2.34}O_{11.34}Tb$	$C_{18}H_{20}N_2O_{11}Tb$
Formula weight	672.37	623.95	599.28
Space group	$P\bar{1}$	$P\bar{1}$	$P\bar{1}$
a/Å	10.5964(10)	10.6610(13)	10.6786(15)
b/Å	11.0355(7)	11.0866(11)	11.0643(14)
c/Å	12.9523(13)	13.1016(15)	13.078(3)
α/°	102.131(7)	100.439(10)	98.788(14)
β/°	112.002(9)	112.923(12)	113.593(18)
γ/°	97.133(6)	98.339(9)	99.692(11)
Volume/Å^3	1338.1(2)	1362.3(3)	1353.7(4)
Z	2	2	2
ρ_{calc} g/cm^3	1.669	1.521	1.470
μ/mm^{-1}	2.706	2.649	2.662
F(000)	670	617	590
Wavelength/Å	0.71420	0.71420	0.71420
2Θ range for data collection/°	3.892 to 56.86	3.864 to 53.02	3.87 to 53.022
Index ranges	$-13 \le h \le 13$, $-14 \le k \le 14$, $-13 \le l \le 13$	$-13 \le h \le 13$, $-13 \le k \le 13$, $-12 \le l \le 12$	$-13 \le h \le 13$, $-13 \le k \le 13$, $-12 \le l \le 12$
Reflections collected	8638	7880	7717
R_{int}, R_{sigma}	$R_{int} = 0.0261$, $R_{sigma} = 0.0406$	$R_{int} = 0.0612$, $R_{sigma} = 0.0743$	$R_{int} = 0.0583$, $R_{sigma} = 0.0961$
Data/restraints/parameters	4465/141/374	4198/146/300	3995/159/300
Goodness of fit on F^2	1.061	1.101	1.192
Final R indexes [I≥2σ(I)]	$R_1 = 0.0416$, $wR_2 = 0.1110$	$R_1 = 0.0996$, $wR_2 = 0.2571$	$R_1 = 0.1225$, $wR_2 = 0.3003$
Final R indexes [all data]	$R_1 = 0.0450$, $wR_2 = 0.1132$	$R_1 = 0.1130$, $wR_2 = 0.2787$	$R_1 = 0.1376$, $wR_2 = 0.3157$
Largest diff. peak/hole / e Å^{-3}	1.86/–1.69	4.37/–2.98	2.89/–3.13
CCDC	1871315	1871314	1871316

Table S3 Selected crystallographic and structure refinement data for **SION-2** in the 100–360 K temperature range on cooling.

Temperature/K	100	120	140	160
Empirical formula	$C_{18}H_{20}N_2O_{11}Tb$	$C_{18}H_{20}N_2O_{11}Tb$	$C_{18}H_{20}N_2O_{11}Tb$	$C_{18}H_{20}N_2O_{11}Tb$
Formula weight	599.28	599.28	599.28	599.28
Space group	$P\bar{1}$	$P\bar{1}$	$P\bar{1}$	$P\bar{1}$
a/Å	10.6219(6)	10.6311(6)	10.6338(6)	10.6385(6)
b/Å	11.1750(5)	11.1791(5)	11.1768(5)	11.1794(5)
c/Å	11.3531(5)	11.3767(5)	11.3943(5)	11.4206(5)
α/°	96.985(4)	96.958(4)	96.944(4)	96.942(4)
β/°	110.840(5)	110.894(5)	110.943(5)	111.003(5)
γ/°	101.422(4)	101.422(4)	101.427(4)	101.423(4)
Volume/Å^3	1207.06(11)	1210.70(11)	1212.21(11)	1215.29(11)
Z	2	2	2	2
ρ_{calc} g/cm^3	1.649	1.644	1.642	1.638
μ/mm^{-1}	3.851	3.839	3.834	3.825
F(000)	590	590	590	590
Wavelength/Å	0.78405	0.78405	0.78405	0.78405
2Θ range for data collection/°	4.196 to 64.432	4.194 to 64.316	4.194 to 64.278	4.194 to 64.498
Index ranges	$-14 \le h \le 14$, $-12 \le k \le 12$, $-14 \le l \le 14$	$-14 \le h \le 14$, $-12 \le k \le 12$, $-14 \le l \le 14$	$-14 \le h \le 14$, $-12 \le k \le 12$, $-14 \le l \le 14$	$-14 \le h \le 14$, $-12 \le k \le 12$, $-14 \le l \le 14$
Reflections collected	6750	6772	6761	6767
R_{int}, R_{sigma}	$R_{int} = 0.0096$, $R_{sigma} = 0.0152$	$R_{int} = 0.0084$, $R_{sigma} = 0.0132$	$R_{int} = 0.0086$, $R_{sigma} = 0.0132$	$R_{int} = 0.0088$, $R_{sigma} = 0.0133$
Data/restraints/parameters	3473/10/292	3474/10/292	3466/10/292	3465/10/292
Goodness of fit on F^2	1.063	1.068	1.069	1.055
Final R indexes [I≥2σ(I)]	$R_1 = 0.0614$, $wR_2 = 0.1632$	$R_1 = 0.0688$, $wR_2 = 0.1812$	$R_1 = 0.0609$, $wR_2 = 0.1662$	$R_1 = 0.0620$, $wR_2 = 0.1674$
Final R indexes [all data]	$R_1 = 0.0629$, $wR_2 = 0.1656$	$R_1 = 0.0705$, $wR_2 = 0.1859$	$R_1 = 0.0627$, $wR_2 = 0.1704$	$R_1 = 0.0635$, $wR_2 = 0.1698$
Largest diff. peak/hole / e Å^{-3}	5.37/−1.52	6.60/−2.17	5.90/−0.79	5.94/−0.83
CCDC	1941013	1941012	1941021	1941015

Temperature/K	180	200	220	240
Empirical formula	$C_{18}H_{20}N_2O_{11}Tb$	$C_{18}H_{20}N_2O_{11}Tb$	$C_{18}H_{20}N_2O_{11}Tb$	$C_{18}H_{20}N_2O_{11}Tb$
Formula weight	599.28	599.28	599.28	599.28
Space group	$P\bar{1}$	$P\bar{1}$	$P\bar{1}$	$P\bar{1}$
a/Å	10.6430(6)	10.6568(6)	10.6410(6)	10.6404(6)
b/Å	11.1747(5)	11.1912(5)	11.1651(5)	11.1598(5)
c/Å	11.4401(6)	11.4798(5)	11.4787(5)	11.4981(5)
α/°	96.900(4)	96.941(4)	96.891(4)	96.878(4)
β/°	111.066(5)	111.109(5)	111.171(5)	111.214(5)
γ/°	101.426(4)	101.425(4)	101.441(4)	101.458(4)
Volume/Å^3	1216.97(12)	1223.96(11)	1218.74(11)	1219.70(11)
Z	2	2	2	2
ρ_{calc} g/cm^3	1.635	1.626	1.633	1.632
μ/mm^{-1}	3.819	3.798	3.814	3.811
F(000)	590	590	590	590
Wavelength/Å	0.78405	0.78405	0.78405	0.78405
2Θ range for data collection/°	4.196 to 64.452	4.19 to 64.326	4.2 to 64.496	4.202 to 64.474
Index ranges	$-14 \le h \le 14$, $-12 \le k \le 12$, $-14 \le l \le 14$	$-14 \le h \le 14$, $-12 \le k \le 12$, $-14 \le l \le 14$	$-14 \le h \le 14$, $-12 \le k \le 12$, $-14 \le l \le 14$	$-14 \le h \le 14$, $-12 \le k \le 12$, $-14 \le l \le 14$
Reflections collected	6784	6812	6812	6812
R_{int}, R_{sigma}	$R_{int} = 0.0085$, $R_{sigma} = 0.0131$	$R_{int} = 0.0094$, $R_{sigma} = 0.0143$	$R_{int} = 0.0087$, $R_{sigma} = 0.0133$	$R_{int} = 0.0100$, $R_{sigma} = 0.0118$
Data/restraints/parameters	3477/34/292	3491/34/292	3496/34/292	3501/34/292
Goodness of fit on F^2	1.092	1.076	1.061	1.053
Final R indexes [I≥2σ(I)]	$R_1 = 0.0771$, $wR_2 = 0.1981$	$R_1 = 0.0880$, $wR_2 = 0.2255$	$R_1 = 0.0683$, $wR_2 = 0.1800$	$R_1 = 0.0833$, $wR_2 = 0.2161$
Final R indexes [all data]	$R_1 = 0.0787$, $wR_2 = 0.2015$	$R_1 = 0.0896$, $wR_2 = 0.2286$	$R_1 = 0.0700$, $wR_2 = 0.1827$	$R_1 = 0.0854$, $wR_2 = 0.2214$
Largest diff. peak/hole / e Å^{-3}	6.77/−2.84	8.36/−2.17	6.32/−1.38	7.08/−2.82
CCDC	1941014	1941016	1941019	1941018

Temperature/K	260	280	300	320
Empirical formula	$C_{18}H_{20}N_2O_{11}Tb$	$C_{18}H_{20}N_2O_{11}Tb$	$C_{18}H_{20}N_2O_{11}Tb$	$C_{18}H_{20}N_2O_{11}Tb$
Formula weight	599.28	599.28	599.28	599.28
Space group	$P\bar{1}$	$P\bar{1}$	$P\bar{1}$	$P\bar{1}$
a/Å	10.6565(6)	10.6648(6)	10.6648(6)	10.6527(6)
b/Å	11.1667(5)	11.1779(5)	11.1682(5)	11.1484(5)
c/Å	11.5332(6)	11.5682(6)	11.5897(6)	11.6012(6)
α/°	96.830(4)	96.856(4)	96.798(4)	96.768(4)
β/°	111.282(5)	111.320(5)	111.386(5)	111.444(5)
γ/°	101.473(4)	101.494(4)	101.528(4)	101.555(5)
Volume/Å^3	1225.53(12)	1230.80(12)	1231.45(12)	1228.51(12)
Z	2	2	2	2
ρ_{calc} g/cm^3	1.624	1.617	1.616	1.62
μ/mm^{-1}	3.793	3.776	3.774	3.783
F(000)	590	590	590	590
Wavelength/Å	0.78405	0.78405	0.78405	0.78405
2Θ range for data collection/°	4.198 to 64.344	4.196 to 64.594	4.2 to 64.572	4.208 to 64.636
Index ranges	$-14 \le h \le 14$, $-12 \le k \le 12$, $-14 \le l \le 14$	$-14 \le h \le 14$, $-12 \le k \le 12$, $-14 \le l \le 14$	$-14 \le h \le 14$, $-12 \le k \le 12$, $-14 \le l \le 15$	$-14 \le h \le 14$, $-12 \le k \le 12$, $-14 \le l \le 15$
Reflections collected	6851	6890	6903	6887
R_{int}, R_{sigma}	$R_{int} = 0.0099$, $R_{sigma} = 0.0150$	$R_{int} = 0.0102$, $R_{sigma} = 0.0149$	$R_{int} = 0.0101$, $R_{sigma} = 0.0148$	$R_{int} = 0.0089$, $R_{sigma} = 0.0136$
Data/restraints/parameters	3518/34/292	3536/34/292	3547/34/292	3536/34/292
Goodness of fit on F^2	1.09	1.067	1.118	1.096
Final R indexes [I≥2σ(I)]	$R_1 = 0.0621$, $wR_2 = 0.1686$	$R_1 = 0.0640$, $wR_2 = 0.1719$	$R_1 = 0.0721$, $wR_2 = 0.1905$	$R_1 = 0.0657$, $wR_2 = 0.1734$
Final R indexes [all data]	$R_1 = 0.0640$, $wR_2 = 0.1715$	$R_1 = 0.0662$, $wR_2 = 0.1759$	$R_1 = 0.0743$, $wR_2 = 0.1940$	$R_1 = 0.0677$, $wR_2 = 0.1765$
Largest diff. peak/hole / e Å^{-3}	5.58/−0.78	5.48/−0.82	6.27/−1.43	5.66/−0.90
CCDC	1941017	1941022	1941025	1941020

Temperature/K	340	360
Empirical formula	$C_{18}H_{20}N_2O_{11}Tb$	$C_{18}H_{20}N_2O_{11}Tb$
Formula weight	599.28	599.28
Space group	$P\bar{1}$	$P\bar{1}$
a/Å	10.6765(7)	10.6634(8)
b/Å	11.1609(5)	11.1405(7)
c/Å	11.6592(6)	11.6932(8)
α/°	96.727(4)	96.751(5)
β/°	111.531(5)	111.604(7)
γ/°	101.573(5)	101.562(6)
Volume/Å^3	1238.03(13)	1237.08(16)
Z	2	2
ρ_{calc} g/cm^3	1.608	1.609
μ/mm^{-1}	3.754	3.757
F(000)	590	590
Wavelength/Å	0.78405	0.78405
2Θ range for data collection/°	4.202 to 64.408	4.21 to 64.656
Index ranges	$-14 \le h \le 14$, $-12 \le k \le 12$, $-15 \le l \le 15$	$-14 \le h \le 14$, $-12 \le k \le 11$, $-15 \le l \le 15$
Reflections collected	6921	6912
R_{int}, R_{sigma}	$R_{int} = 0.0093$, $R_{sigma} = 0.0143$	$R_{int} = 0.0121$, $R_{sigma} = 0.0180$
Data/restraints/parameters	3566/34/292	3565/60/291
Goodness of fit on F^2	1.052	1.093
Final R indexes [I≥2σ(I)]	$R_1 = 0.0680$, $wR_2 = 0.1785$	$R_1 = 0.0748$, $wR_2 = 0.1937$
Final R indexes [all data]	$R_1 = 0.0701$, $wR_2 = 0.1821$	$R_1 = 0.0771$, $wR_2 = 0.1974$
Largest diff. peak/hole / e Å^{-3}	5.61/−0.77	6.20/−1.15
CCDC	1941023	1941024

Section S1. Quantum ESPRESSO input file for periodic density functional theory (DFT) calculations.

```
&control
  calculation = 'vc-relax'
  restart_mode = 'from_scratch'
  wf_collect=.TRUE.
  verbosity = 'high'
  outdir = './'
  etot_conv_thr = 1.0d-05
  forc_conv_thr = 1.0d-04
  nstep=1000
/
&system
  ibrav = 0
  nat = 104
  ntyp = 6
  tot_charge = 0.0
  ecutwfc = 120
  ecutrho = 500
  vdw_corr = 'grimme-d2'
  nosym = .TRUE.
  nspin = 2
  tot_magnetization = 4
  starting_magnetization(1)=0.5
  starting_magnetization(2)=-0.5
/
&electrons
  scf_must_converge = .false.
  electron_maxstep = 80
  conv_thr = 1.0d-06
  mixing_mode='local-TF'
  mixing_beta = 0.5
  diagonalization = 'david'
/
&ions
ion_dynamics = 'bfgs'
/
&cell
cell_dynamics='bfgs'
cell_dofree='all'
press = 0.0
press_conv_thr = 1.0d-01
/

K_POINTS gamma

ATOMIC_SPECIES
 Tb1 158.930 Tb.pbe-spdfn-kjpaw_psl.1.0.0.UPF
 Tb2 158.930 Tb.pbe-spdfn-kjpaw_psl.1.0.0.UPF
  O 15.999 O.pbe-n-kjpaw_psl.1.0.0.UPF
  H 1.008 H.pbe-kjpaw_psl.1.0.0.UPF
  C 12.010 C.pbe-n-kjpaw_psl.1.0.0.UPF
  N 14.007 N.pbe-n-kjpaw_psl.1.0.0.UPF

CELL_PARAMETERS angstrom
  10.53200    0.00000    0.00000
  -1.23968   10.92288    0.00000
  -4.51256   -3.57023   11.41582

ATOMIC_POSITIONS crystal
Tb1            0.60404    0.54723    0.68227
O             -0.33641    0.49485    0.52296
O              0.48535    0.33544    0.58655
```

O	0.42801	0.27662	0.39463
O	-0.17127	-0.31081	-0.21822
O	-0.37527	0.43314	0.33650
O	-0.32467	-0.24670	-0.15226
O	0.56970	0.47806	0.83636
O	-0.17543	0.40297	0.26815
H	-0.25676	0.39860	0.26001
C	0.46340	0.25591	0.49201
O	0.45513	0.05234	0.29164
H	0.48534	0.12839	0.30266
O	-0.26354	-0.01412	-0.00407
H	-0.30877	-0.08823	-0.03125
O	0.77137	0.42256	0.74510
C	-0.09123	0.45129	0.38407
C	-0.29398	0.46918	0.44162
C	-0.10216	-0.10991	-0.07492
C	0.47957	0.12201	0.49344
C	-0.14264	0.48549	0.47084
C	0.49823	-0.08824	0.40499
H	0.49694	-0.14864	0.33966
C	-0.20410	-0.22783	-0.15292
C	-0.04997	0.53299	0.58569
H	-0.08345	0.55504	0.64435
C	-0.13625	-0.01201	-0.00491
C	0.03352	-0.09721	-0.06900
H	0.05621	-0.16294	-0.11529
C	0.47814	0.03017	0.39683
N	0.93627	0.32625	0.82805
N	0.50027	0.31130	0.89147
C	0.48222	0.38545	0.82494
H	0.39606	0.36757	0.76324
C	0.87210	0.41086	0.79166
H	0.93599	0.48738	0.81388
C	0.39483	0.20810	0.87578
H	0.31429	0.19991	0.80683
H	0.37067	0.22447	0.94277
H	0.42815	0.13007	0.86709
C	0.87908	0.19814	0.80299
H	0.86632	0.18356	0.87010
H	0.94032	0.14698	0.78366
H	0.79086	0.17483	0.73781
C	0.62350	0.33054	0.98716
H	0.69402	0.30580	0.96052
H	0.60969	0.27961	1.03528
H	0.65219	0.41954	1.03198
C	1.08565	0.36476	0.89681
H	1.10468	0.36204	0.97530
H	1.11899	0.45042	0.89844
H	1.13168	0.30718	0.86198
Tb2	0.39596	0.45277	0.31773
O	0.33641	0.50515	0.47704
O	0.51465	-0.33544	0.41345
O	0.57199	-0.27662	0.60537
O	0.17127	0.31081	0.21822
O	0.37527	0.56686	0.66350
O	0.32467	0.24670	0.15226
O	0.43030	0.52194	0.16364
O	0.17543	0.59703	0.73185
H	0.25676	0.60140	0.73999
C	0.53660	-0.25591	0.50799
O	0.54487	-0.05234	0.70836
H	0.51466	-0.12839	0.69734
O	0.26354	0.01412	0.00407

H	0.30877	0.08823	0.03125
O	0.22863	0.57744	0.25490
C	0.09123	0.54871	0.61593
C	0.29398	0.53082	0.55839
C	0.10216	0.10991	0.07492
C	0.52043	-0.12202	0.50656
C	0.14264	0.51451	0.52916
C	0.50177	0.08824	0.59501
H	0.50306	0.14864	0.66034
C	0.20410	0.22783	0.15292
C	0.04997	0.46701	0.41431
H	0.08345	0.44497	0.35565
C	0.13625	0.01201	0.00491
C	-0.03352	0.09721	0.06900
H	-0.05621	0.16294	0.11529
C	0.52185	-0.03017	0.60317
N	0.06373	0.67375	0.17195
N	0.49973	0.68870	0.10853
C	0.51778	0.61455	0.17506
H	0.60394	0.63243	0.23676
C	0.12790	0.58914	0.20834
H	0.06401	0.51263	0.18612
C	0.60517	0.79190	0.12422
H	0.68571	0.80009	0.19317
H	0.62933	0.77553	0.05723
H	0.57185	0.86993	0.13291
C	0.12092	0.80186	0.19701
H	0.13368	0.81644	0.12990
H	0.05968	0.85302	0.21634
H	0.20914	0.82517	0.26219
C	0.37649	0.66946	0.01284
H	0.30598	0.69420	0.03948
H	0.39031	0.72039	-0.03528
H	0.34781	0.58046	-0.03198
C	-0.08565	0.63524	0.10319
H	-0.10468	0.63796	0.02470
H	-0.11899	0.54958	0.10156
H	-0.13168	0.69282	0.13802

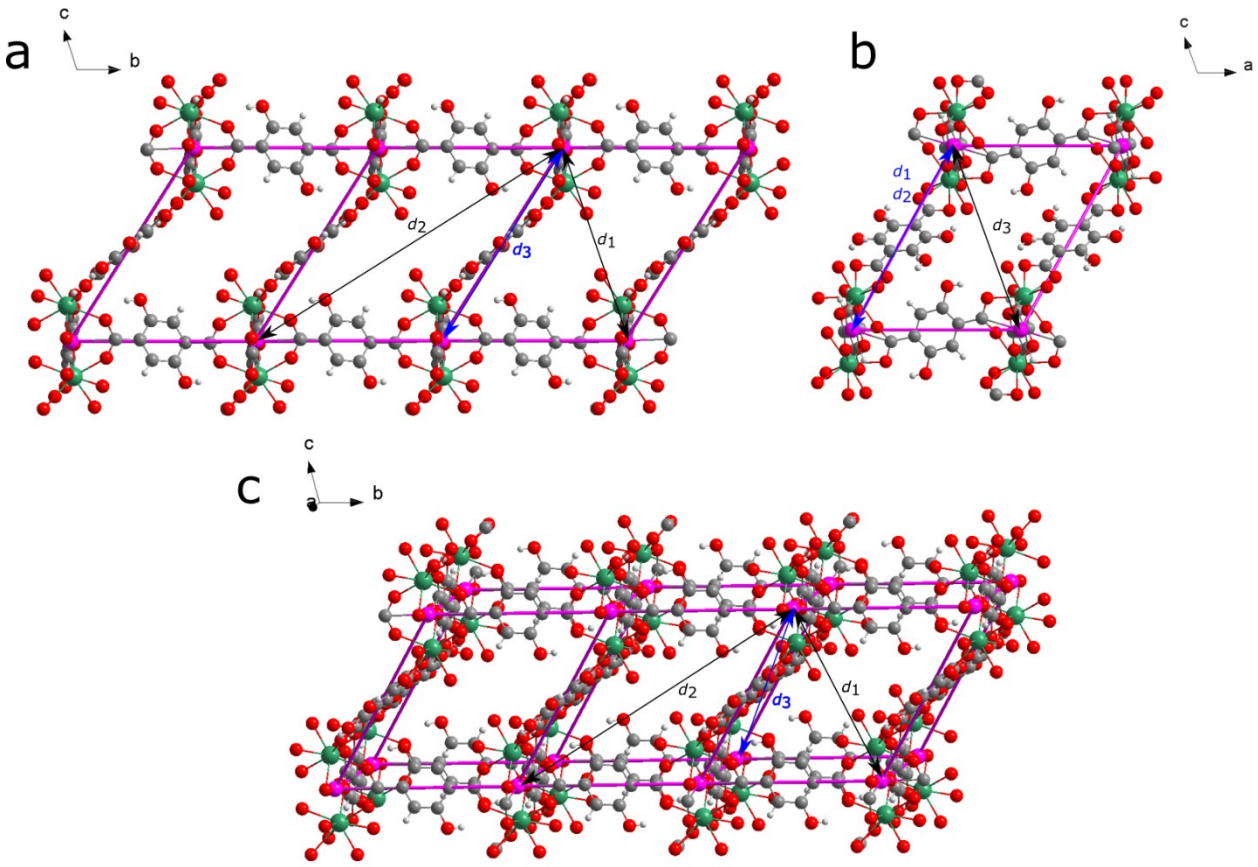

Fig. S1 Crystal structure of **SION-2** overlaid with its topological description. Tb_2 clusters act as 6-coordinated nodes, while $DHBDC^{2-}$ ligands are 2-coordinating links. Distances d_1, d_2, and d_3, localised within the crystal structure of **SION-2** are approximately collinear with the principal axes X_1, X_2, and X_3 respectively, markedly different from the crystallographic axes *a*, *b*, and *c*. Distances d_1, d_2, and d_3 marked in black are in the plane of the picture, while those marked in blue extend out of that plane. (a) View along *a*-axis, (b) View along *b*-axis (c) View along an intermediate direction. Coordinated and non-coordinated DMF molecules have been omitted for clarity.

Table S4 Edge lengths, angles, and volumes of the triclinic unit cell of **SION-2** determined from SCXRD measurements in the 100–340 K temperature range.

T (K)	a (Å)	b (Å)	c (Å)	α (°)	β (°)	γ (°)	V (Å^3)
100	10.5096(6)	10.9768(4)	12.5019(6)	104.759(4)	107.340(5)	97.380(4)	1298.23(12)
120	10.5156(6)	10.9858(4)	12.5290(6)	104.707(4)	107.578(5)	97.265(4)	1301.80(12)
140	10.4937(6)	10.9559(4)	12.5321(6)	104.652(4)	107.923(4)	97.114(4)	1294.06(12)
160	10.5194(6)	10.9889(4)	12.5734(6)	104.589(4)	108.172(5)	96.992(4)	1304.34(12)
180	10.5256(6)	10.9947(5)	12.6032(6)	104.523(4)	108.540(5)	96.829(4)	1306.91(13)
200	10.5213(5)	10.9954(5)	12.6323(5)	104.438(4)	108.872(4)	96.664(4)	1307.93(11)
220	10.5190(6)	10.9933(5)	12.6565(5)	104.317(4)	109.262(4)	96.536(4)	1307.83(12)
240	10.5121(6)	10.9835(5)	12.6782(5)	104.175(4)	109.639(4)	96.452(4)	1305.96(12)
260	10.5371(6)	11.0161(5)	12.7345(5)	104.005(5)	109.918(4)	96.448(4)	1317.37(12)
280	10.5333(6)	11.0035(5)	12.7511(5)	103.784(5)	110.271(4)	96.437(4)	1315.34(12)
300	10.5445(7)	11.0141(6)	12.7860(8)	103.484(6)	110.657(6)	96.517(5)	1319.52(16)
320	10.5861(8)	11.0497(6)	12.8741(9)	103.021(6)	111.134(7)	96.698(5)	1335.67(19)
340	10.5964(10)	11.0355(7)	12.9523(13)	102.131(7)	112.002(9)	97.133(6)	1338.1(2)

Table S5 Coefficients α of thermal expansion determined experimentally along three principal axes X_1, X_2, and X_3 of the crystals of **SION-2** in the 100–340 K temperature range. The simultaneous volumetric coefficient of thermal expansion is α_V = +144(16) MK^{-1}.

Axis	Direction	α (MK^{-1})
X_1	$[0.83\ 0.13\ 0.54] \cong [5\bar{1}3]$	–153(6)
X_2	$[0.34\ 0.89\ 0.29] \cong [131]$	+43(6)
X_3	$[0.58\ 0.07\ 0.81] \cong [\bar{2}03]$	+230(20)

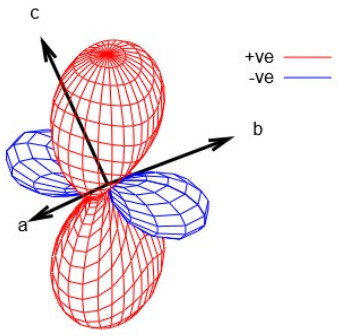

Fig. S2 Graphical representation of the coefficients of thermal expansion of **SION-2** in the form of an expansivity indicatrix.

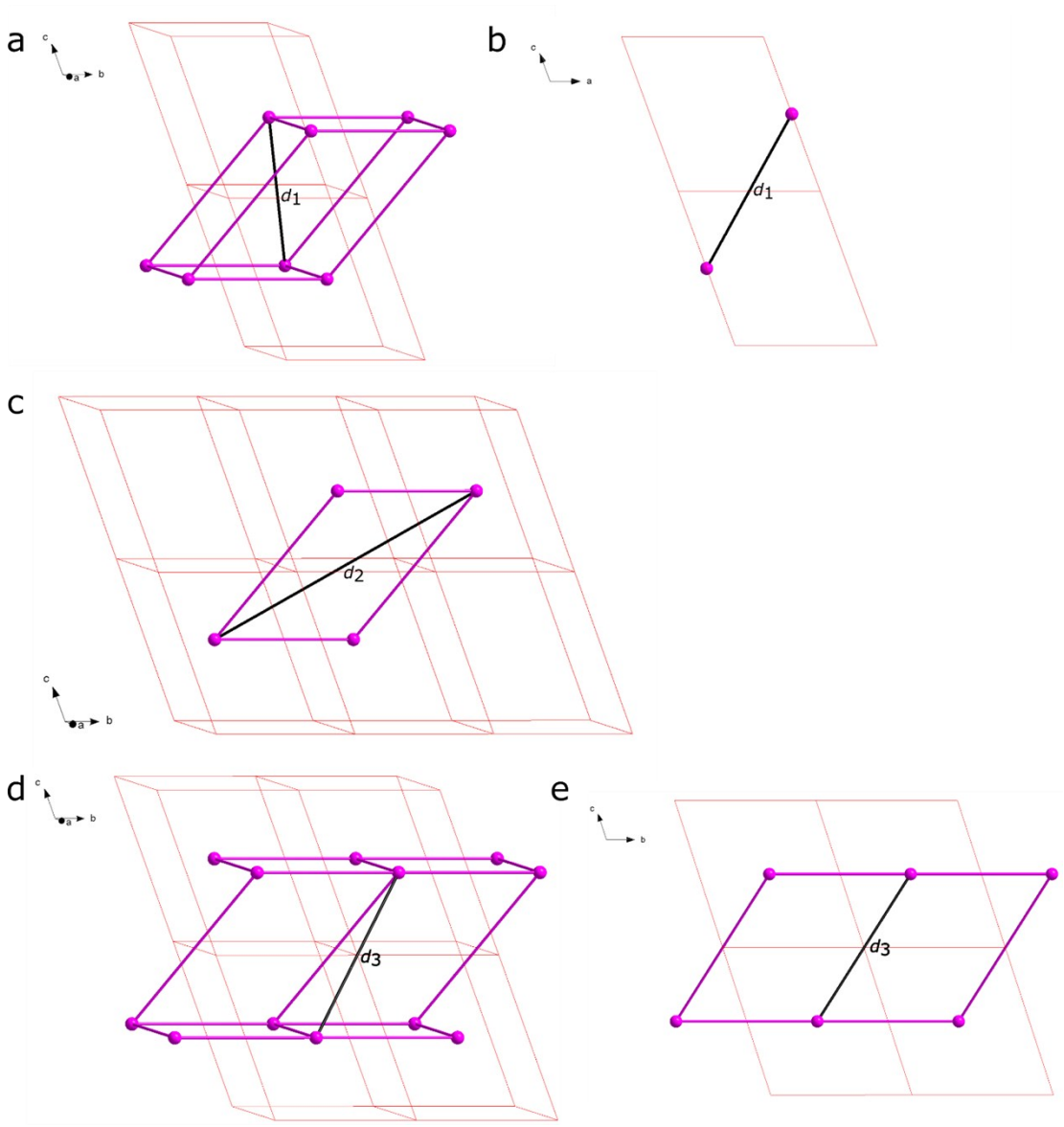

Fig. S3 (a) Localisation of the distance d_1 within the unit cell of **SION-2**. (b) From the projection onto the *ac* plane (both nodes involved are situated at $y = 0.5$) and the law of cosines it is inferred that $d_1 = \sqrt{a^2 + c^2 - 2ac\ cos(180° - \beta)}$ (c) Localisation of the distance d_2 within the unit cell of **SION-2**. This distance is not parallel to any face of the unit cell, so in order to calculate its value the general formula for the interstitial distance can only be applied $d_2 = \sqrt{a^2 + 4b^2 + c^2 + 4ab\cos\gamma + 4bc\cos\alpha + 2ac\cos\beta}$ (d) Localisation of the distance d_3 within the unit cell of **SION-2**. (e) From the projection onto the *bc* plane (both nodes involved are situated at $x = 0$) and the law of cosines it is inferred that $d_3 = \sqrt{b^2 + c^2 - 2bc\ cos(180° - \alpha)}$

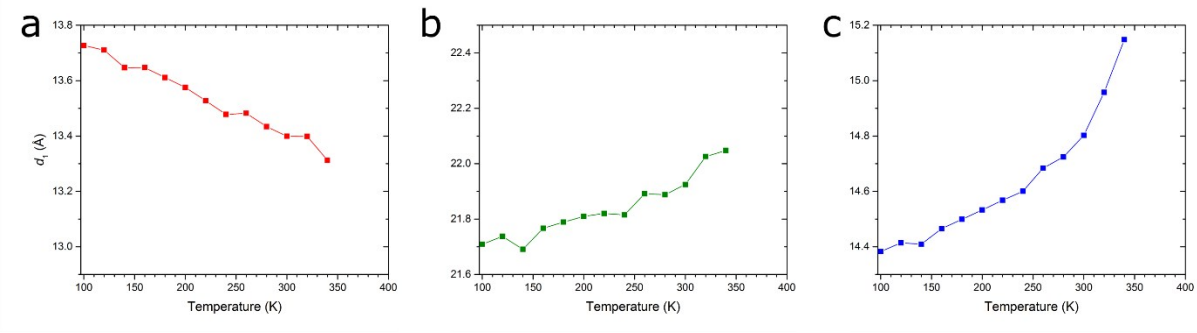

Fig. S4 Change of the absolute values of the distances (a) d_1, (b) d_2, and (c) d_3 as a function of temperature.

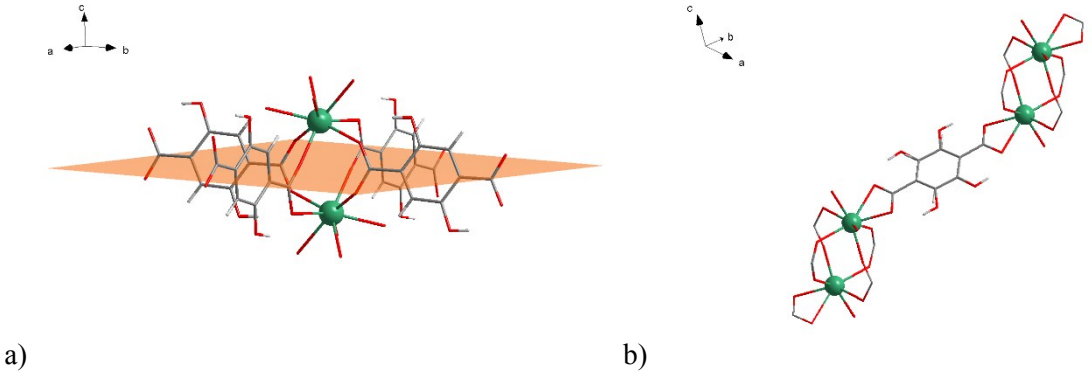

a) b)

Fig. S5 (a) A Tb^{III}_2 unit bound simultaneously to four $DHBDC^{2-}$ ligands via O2,O4- and O3,O6-bridging endowing the 2-dimensional planes (marked in orange) with an inflexibility. (b) η^2-chelating $DHBDC^{2-}$ ligands, the position of which with respect to the Tb^{III}_2 cluster is not constrained.

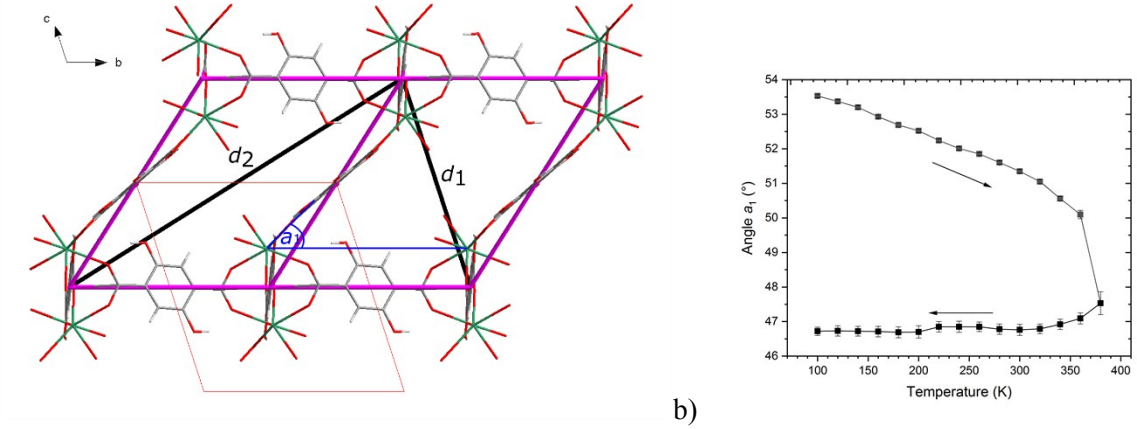

a) b)

Fig. S6 (a) Angle a_1 representing the inclination of the η^2-chelating $DHBDC^{2-}$ ligands with respect to the rigid Tb^{III}–bridging $DHBDC^{2-}$ planes. (b) Progression of a_1 as a function of temperature. The arrows indicate the heating and the cooling regime.

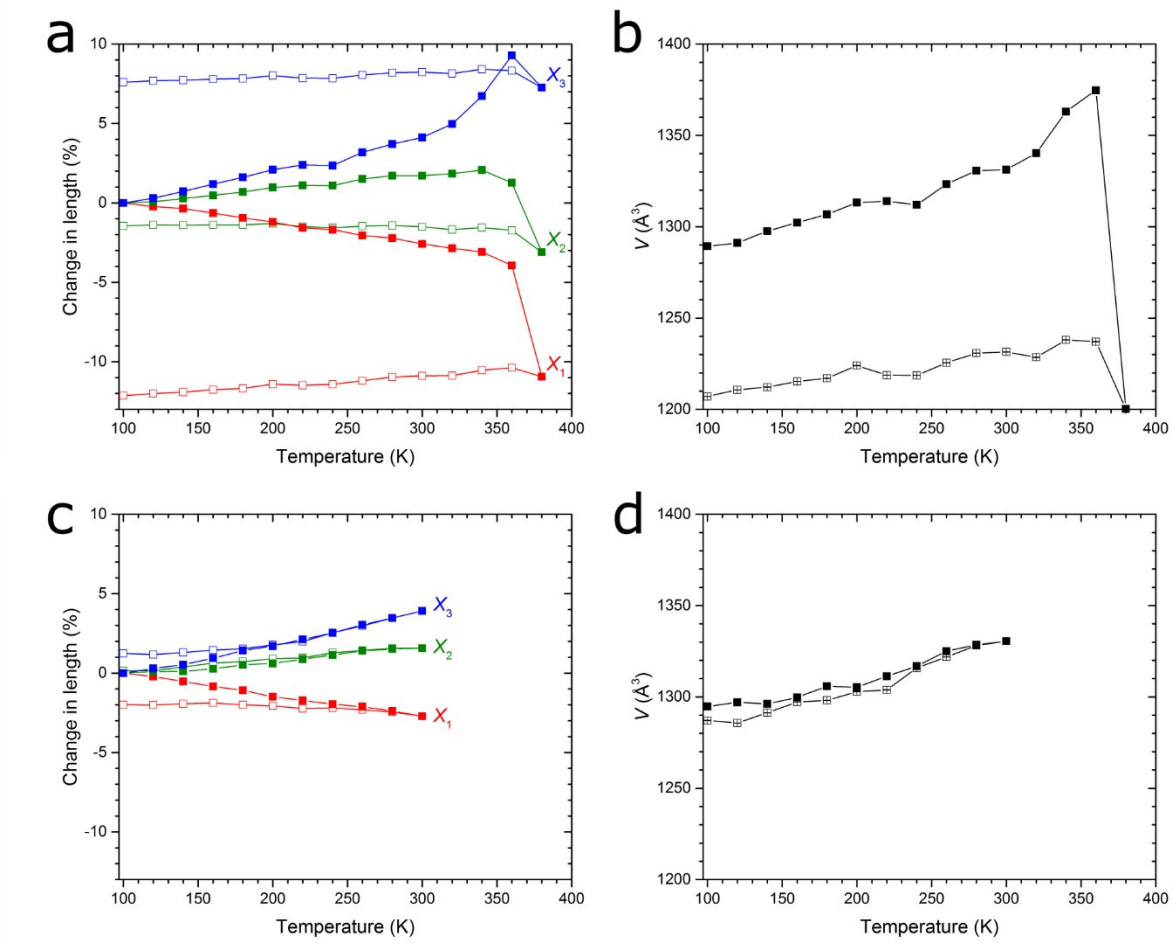

Fig. S7 (a) Percentage change in lengths of the principal axes X_1, X_2, and X_3 and (b) absolute change of the unit-cell volume of **SION-2** in the 100–380–100 K temperature range. (c) Percentage change in lengths of the principal axes X_1, X_2, and X_3 and (d) absolute change of the unit-cell volume of **SION-2** in the 100–300–100 K temperature range. Full symbols denote the heating, while the empty ones – the cooling regime.

Table S6 Edge lengths, angles, and volumes of the triclinic unit cell of **SION-2** determined from SCXRD measurements in the 100–380–100 K temperature range on heating and cooling.

T (K)	*a* (Å)	*b* (Å)	*c* (Å)	*α* (°)	*β* (°)	*γ* (°)	*V* (Å^3)
100	10.4740(6)	10.9218(3)	12.5171(6)	104.803(4)	107.218(5)	97.441(4)	1289.29(12)
120	10.4785(6)	10.9262(3)	12.5373(6)	104.797(4)	107.481(5)	97.272(4)	1291.14(12)
140	10.4969(6)	10.9385(6)	12.5755(6)	104.753(4)	107.766(5)	97.097(4)	1297.59(12)
160	10.5112(6)	10.9539(3)	12.6033(6)	104.720(4)	108.142(5)	96.856(4)	1302.25(12)
180	10.5222(6)	10.9713(3)	12.6332(6)	104.684(4)	108.521(5)	96.635(4)	1306.79(12)
200	10.5396(6)	10.9909(3)	12.6702(6)	104.581(4)	108.915(5)	96.463(4)	1313.17(12)
220	10.5391(6)	10.9954(3)	12.6924(6)	104.471(4)	109.276(5)	96.350(4)	1313.97(12)
240	10.5332(6)	10.9940(3)	12.6843(6)	104.463(4)	109.319(5)	96.339(4)	1311.94(12)
260	10.5588(6)	11.0205(3)	12.7641(6)	104.174(4)	109.941(5)	96.235(4)	1323.30(12)
280	10.5792(6)	11.0356(4)	12.8087(7)	103.932(4)	110.274(5)	96.262(4)	1330.70(13)
300	10.5785(6)	11.0332(4)	12.8359(7)	103.661(4)	110.638(5)	96.324(4)	1331.17(13)
320	10.6017(6)	11.0500(4)	12.9005(7)	103.241(4)	111.115(5)	96.457(4)	1340.32(13)
340	10.659(6)	11.1024(5)	13.0304(7)	102.405(4)	111.874(5)	96.904(5)	1363.06(13)
360	10.6975(7)	11.1103(5)	13.1588(7)	100.742(4)	112.996(6)	98.049(5)	1374.72(16)
380	10.5363(13)	11.0128(19)	11.6445(19)	96.840(14)	111.826(13)	101.636(12)	1200.2(4)
360	10.6634(8)	11.1405(7)	11.6932(8)	96.751(5)	111.604(7)	101.562(6)	1237.09(17)
340	10.6765(7)	11.1609(5)	11.6592(6)	96.727(4)	111.531(5)	101.572(5)	1238.04(14)
320	10.6527(6)	11.1484(5)	11.6012(6)	96.768(4)	111.444(5)	101.555(5)	1228.50(13)
300	10.6648(6)	11.1682(5)	11.5897(6)	96.799(4)	111.386(5)	101.528(4)	1231.44(13)
280	10.6648(6)	11.1779(5)	11.5682(6)	96.856(4)	111.320(5)	101.494(4)	1230.79(13)
260	10.6565(6)	11.1667(5)	11.5332(6)	96.830(4)	111.282(5)	101.473(4)	1225.52(12)
240	10.6376(6)	11.1560(5)	11.4941(5)	96.866(4)	111.213(5)	101.459(4)	1218.61(12)
220	10.6410(6)	11.1651(5)	11.4787(5)	96.891(4)	111.171(5)	101.441(4)	1218.75(12)
200	10.6568(6)	11.1912(5)	11.4798(5)	96.941(4)	111.109(5)	101.425(4)	1223.97(12)
180	10.6430(6)	11.1747(5)	11.4401(5)	96.900(4)	111.066(5)	101.426(4)	1216.96(12)
160	10.6385(6)	11.1794(5)	11.4206(5)	96.941(4)	111.003(5)	101.423(4)	1215.30(12)
140	10.6338(6)	11.1768(5)	11.3943(5)	96.944(4)	110.943(5)	101.428(4)	1212.19(12)
120	10.6311(6)	11.1791(5)	11.3767(5)	96.958(4)	110.894(5)	101.421(4)	1210.69(12)
100	10.6219(6)	11.1750(5)	11.3531(5)	96.985(4)	110.840(5)	101.422(4)	1207.05(12)

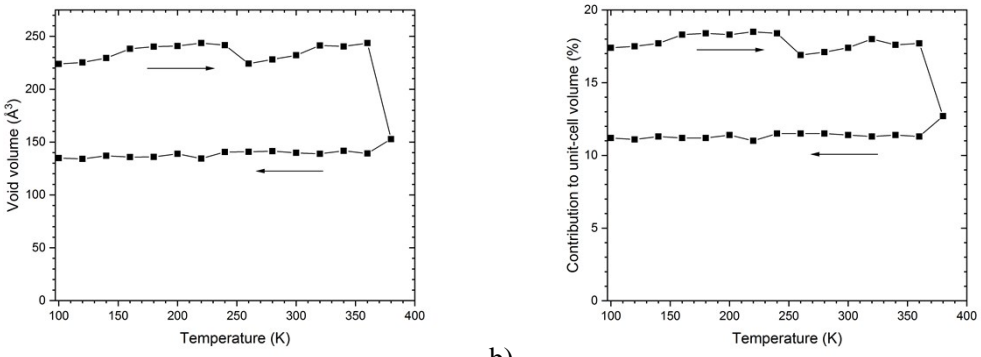

a) b)

Fig. S8 Volume of the structural voids found in the crystal structure of **SION-2** expressed (a) as absolute values (in Å^3) and (b) as a contribution to the overall unit-cell volume. Void volume was calculated by the VOIDS procedure of the program MERCURY. In the 100–340 K temperature range on heating, non-coordinated DMF molecules were manually removed before running the void volume calculation. The arrows indicate the heating and the cooling regime.

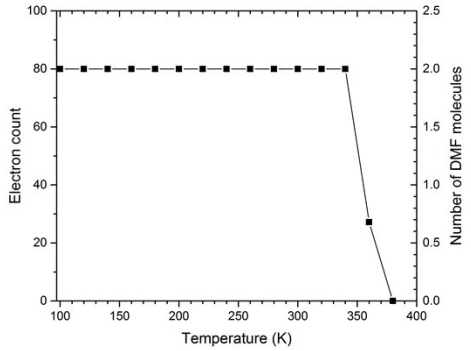

Fig. S9 Content of the structural voids of **SION-2** plotted against temperature (in K) expressed in terms of integrated electron density. Electron count of 80 e$^-$ (full occupancy of two DMF molecules per unit cell) was arbitrarily assigned to all temperatures up to 340 K, while last two data points were quantified with the SQUEEZE algorithm within the PLATON program suite.

Table S7 Mechanical properties of **SION-2**: full stiffness tensor C_{ij}, bulk modulus K, shear modulus G, Young's modulus E, anisotropy of Young's modulus A_E (defined as E_{max}/E_{min}), and linear compressibility β. The values of bulk and shear moduli are reported as Voigt-Reuss-Hill averages, while Young's modulus and linear compressibility are reported in terms of their minimum and maximum values (for the full 3D representations see Fig. 3 in the main text).

Property	Value
$\begin{bmatrix} C_{11} & C_{12} & C_{13} & C_{14} & C_{15} & C_{16} \\ & C_{22} & C_{23} & C_{24} & C_{25} & C_{26} \\ & & C_{33} & C_{34} & C_{35} & C_{36} \\ & & & C_{44} & C_{45} & C_{46} \\ & & & & C_{55} & C_{56} \\ & & & & & C_{66} \end{bmatrix} (GPa)$	$\begin{bmatrix} 20.5 & 8.6 & 2.0 & -1.0 & 0.2 & -1.0 \\ & 19.3 & 2.1 & 0.3 & -1.0 & 0.0 \\ & & 12.9 & 0.5 & -1.0 & 0.0 \\ & & & 1.1 & 0.4 & -0.4 \\ & & & & 1.1 & 0.4 \\ & & & & & 1.1 \end{bmatrix}$
$K(GPa)$	7.1
$G(GPa)$	1.8
$E_{min}(GPa)$	0.15
$E_{max}(GPa)$	14.8
A_E	103
$\beta_{min}(TPa^{-1})$	–284
$\beta_{max}(TPa^{-1})$	+605

Table S8 Edge lengths, angles, and volumes of the triclinic unit cell of **SION-2** determined from SCXRD measurements in the 100–300–100 K temperature range on heating and cooling.

T (K)	a (Å)	b (Å)	c (Å)	α (°)	β (°)	γ (°)	V (Å^3)
100	10.4901(6)	10.9330(4)	12.5332(6)	104.772(4)	107.209(5)	97.408(4)	1294.77(12)
120	10.4964(6)	10.9385(4)	12.5536(6)	104.754(4)	107.472(5)	97.243(4)	1297.06(12)
140	10.4935(6)	10.9365(4)	12.5654(6)	104.745(4)	107.751(5)	97.071(4)	1296.23(12)
160	10.5049(6)	10.9483(4)	12.5894(6)	104.711(4)	108.121(5)	96.845(4)	1299.70(12)
180	10.5212(6)	10.9697(4)	12.6243(6)	104.673(4)	108.498(5)	96.634(4)	1305.86(12)
200	10.5170(6)	10.9737(4)	12.6400(7)	104.625(4)	108.862(5)	96.467(4)	1305.32(13)
220	10.5312(7)	10.9923(4)	12.6777(7)	104.523(4)	109.210(5)	96.348(4)	1311.33(14)
240	10.5442(7)	11.0078(4)	12.7133(7)	104.373(4)	109.552(5)	96.258(5)	1316.85(14)
260	10.5653(7)	11.0256(4)	12.7629(7)	104.186(4)	109.902(6)	96.216(5)	1325.00(14)
280	10.5735(7)	11.0298(5)	12.7995(8)	103.973(4)	110.249(6)	96.219(5)	1328.50(15)
300	10.5777(7)	11.0325(5)	12.8313(7)	103.730(4)	110.611(6)	96.270(5)	1330.55(15)
280	10.5752(7)	11.0347(4)	12.7898(7)	103.907(4)	110.295(6)	96.254(5)	1328.15(14)
260	10.5621(7)	11.0272(5)	12.7404(7)	104.100(4)	109.996(6)	96.262(5)	1321.94(14)
240	10.5494(7)	11.0166(5)	12.6931(7)	104.218(4)	109.725(6)	96.289(5)	1315.81(14)
220	10.5180(7)	10.9930(5)	12.6295(7)	104.362(4)	109.454(5)	96.321(5)	1303.87(14)
200	10.5216(7)	10.9951(5)	12.5999(7)	104.415(4)	109.242(5)	96.365(5)	1302.88(14)
180	10.5127(7)	10.9902(5)	12.5596(7)	104.502(4)	109.035(5)	96.406(5)	1298.11(14)
160	10.5162(7)	10.9943(5)	12.5325(7)	104.547(4)	108.870(5)	96.440(5)	1297.23(14)
140	10.5041(6)	10.9869(5)	12.4908(7)	104.614(4)	108.718(5)	96.465(5)	1291.33(14)
120	10.4901(6)	10.9817(5)	12.4553(7)	104.682(4)	108.602(5)	96.492(5)	1285.72(14)
100	10.4999(6)	10.9917(5)	12.4405(7)	104.682(4)	108.544(5)	96.491(5)	1287.09(15)

References

1. K. V. K. Rao, S. V. N. Naidu and K. S. Murthy, *J. Phys. Chem. Solids*, 1968, **29**, 245-248.
2. J. B. Nelson and D. P. Riley, *P. Phys. Soc.*, 1945, **57**, 477-486.
3. G. Beckman and R. Kiessling, *Nature*, 1956, **178**, 1341.
4. T. A. Mary, J. S. O. Evans, T. Vogt and A. W. Sleight, *Science*, 1996, **272**, 90-92.
5. N. Lock, Y. Wu, M. Christensen, L. J. Cameron, V. K. Peterson, A. J. Bridgeman, C. J. Kepert and B. B. Iversen, *J. Phys. Chem. C*, 2010, **114**, 16181-16186.
6. A. L. Goodwin and C. J. Kepert, *Phys. Rev. B*, 2005, **71**, 140301.
7. Y. Wu, A. Kobayashi, G. J. Halder, V. K. Peterson, K. W. Chapman, N. Lock, P. D. Southon and C. J. Kepert, *Angew. Chem., Int. Ed.*, 2008, **47**, 8929-8932.
8. Y. Wu, V. K. Peterson, E. Luks, T. A. Darwish and C. J. Kepert, *Angew. Chem.*, 2014, **53**, 5175-5178.
9. J. S. O. Evans, T. A. Mary and A. W. Sleight, *J. Solid State Chem.*, 1998, **137**, 148-160.
10. Z. Liu, Q. Li, H. Zhu, K. Lin, J. Deng, J. Chen and X. Xing, *Chem. Commun.*, 2018, **54**, 5712-5715.
11. B. K. Greve, K. L. Martin, P. L. Lee, P. J. Chupas, K. W. Chapman and A. P. Wilkinson, *J. Am. Chem. Soc.*, 2010, **132**, 15496-15498.
12. J. Chen, Q. Gao, A. Sanson, X. Jiang, Q. Huang, A. Carnera, C. G. Rodriguez, L. Olivi, L. Wang, L. Hu, K. Lin, Y. Ren, Z. Lin, C. Wang, L. Gu, J. Deng, J. P. Attfield and X. Xing, *Nat. Commun.*, 2017, **8**, 14441.
13. S. E. Tallentire, F. Child, I. Fall, L. Vella-Zarb, I. Radosavljević Evans, M. G. Tucker, D. A. Keen, C. Wilson and J. S. O. Evans, *J. Am. Chem. Soc.*, 2013, **135**, 12849-12856.
14. W. Yao, X. Jiang, R. Huang, W. Li, C. Huang, Z. Lin, L. Li and C. Chen, *Chem. Commun.*, 2014, **50**, 13499-13501.
15. G. Shirane and S. Hoshino, *J. Phys. Soc. Jpn.*, 1951, **6**, 265-270.
16. K. S. Knight, *J. Miner. Petrol. Sci.*, 2014, **109**, 118-124.
17. I. E. Collings, A. B. Cairns, A. L. Thompson, J. E. Parker, C. C. Tang, M. G. Tucker, J. Catafesta, C. Levelut, J. Haines, V. Dmitriev, P. Pattison and A. L. Goodwin, *J. Am. Chem. Soc.*, 2013, **135**, 7610-7620.
18. E. Pachoud, J. Cumby, C. T. Lithgow and J. P. Attfield, *J. Am. Chem. Soc.*, 2018, **140**, 636-641.
19. A. L. Goodwin, K. W. Chapman and C. J. Kepert, *J. Am. Chem. Soc.*, 2005, **127**, 17980-17981.
20. A. E. Phillips, A. L. Goodwin, G. J. Halder, P. D. Southon and C. J. Kepert, *Angew. Chem., Int. Ed.*, 2008, **120**, 1396 -1399.
21. Q. Gao, J. Chen, Q. Sun, D. Chang, Q. Huang, H. Wu, A. Sanson, R. Milazzo, H. Zhu, Q. Li, Z. Liu, J. Deng and X. Xing, *Angew. Chem., Int. Ed.*, 2017, **56**, 9023-9028.
22. S. G. Duyker, V. K. Peterson, G. J. Kearley, A. J. Ramirez-Cuesta and C. J. Kepert, *Angew. Chem.*, 2013, **125**, 5374-5378.
23. S. J. Hibble, A. M. Chippindale, A. H. Pohl and A. C. Hannon, *Angew. Chem., Int. Ed.*, 2007, **46**, 7116-7118.
24. M. P. Attfield and A. W. Sleight, *Chem. Mater.*, 1998, **10**, 2013-2019.
25. D. A. Woodcock, P. Lightfoot, P. A. Wright, L. A. Villaescusa, M.-J. Díaz-Cabañas and M. A. Camblor, *J. Mater. Chem.*, 1999, **9**, 349-351.
26. D. A. Woodcock, P. Lightfoot, L. A. Villaescusa, M.-J. Díaz-Cabañas, M. A. Camblor and D. Engberg, *Chem. Mater.*, 1999, **11**, 2508-2514.
27. P. Lightfoot, D. A. Woodcock, M. J. Maple, L. A. Villaescusa and P. A. Wright, *J. Mater. Chem.*, 2001, **11**, 212-216.
28. I. Bull, P. Lightfoot, L. A. Villaescusa, L. M. Bull, R. K. B. Gover, J. S. O. Evans and R. E. Morris, *J. Am. Chem. Soc.*, 2003, **125**, 4342-4349.
29. L. Leardini, S. Quartieri, G. Vezzalini and R. Arletti, *Micropor. Mesopor. Mater.*, 2015, **202**, 226-233.

30. D. Santamaría-Pérez, T. Marqueño, S. MacLeod, J. Ruiz-Fuertes, D. Daisenberger, R. Chuliá-Jordan, D. Errandonea, J. L. Jordá, F. Rey, C. McGuire, A. Mahkluf, A. Kavner and C. Popescu, *Chem. Mater.*, 2017, **29**, 4502-4510.
31. A. Dosen and B. A. Marinkovic, *Bull. Mater. Sci.*, 2019, **42**, 86.
32. W. G. Marshall, R. H. Jones and K. S. Knight, *CrystEngComm*, 2018, **20**, 3246-3250.
33. A. L. Goodwin, M. Calleja, M. J. Conterio, M. T. Dove, J. S. O. Evans, D. A. Keen, L. Peters and M. G. Tucker, *Science*, 2008, **319**, 794-797.
34. J. M. Ogborn, I. E. Collings, S. A. Moggach, A. L. Thompson and A. L. Goodwin, *Chem. Sci.*, 2012, **3**, 3011-3017.
35. T.-M. Zhao, S. Chen, R. Shang, B.-W. Wang, Z.-M. Wang and S. Gao, *Inorg. Chem.*, 2016, **55**, 10075-10082.
36. J. Kusz, M. Zubko, A. Fitch and P. Gütlich, *Z. Kristallogr.*, 2011, **226**, 576-584.
37. A. B. Cairns, A. L. Thompson, M. G. Tucker, J. Haines and A. L. Goodwin, *J. Am. Chem. Soc.*, 2012, **134**, 4454-4456.
38. I. E. Collings, M. G. Tucker, D. A. Keen and A. L. Goodwin, *CrystEngComm*, 2014, **16**, 3498-3506.
39. R. K. Das, H. Aggarwal and L. J. Barbour, *Inorg. Chem.*, 2015, **54**, 8171-8173.
40. S. A. Hodgson, J. Adamson, S. J. Hunt, M. J. Cliffe, A. B. Cairns, A. L. Thompson, M. G. Tucker, N. P. Funnell and A. L. Goodwin, *Chem. Commun.*, 2014, **50**, 5264-5266.
41. Z. Zhang, X. Jiang, G. Feng, Z. Lin, B. Hu and W. Li, *J. Solid State Chem.*, 2016, **233**, 289-293.
42. J. Pang, C. Liu, Y. Huang, M. Wu, F. Jiang, D. Yuan, F. Hu, K. Su, G. Liu and M. Hong, *Angew. Chem., Int. Ed.*, 2016, **55**, 7478-7482.
43. Z. Liu, C. Liu, Q. Li, J. Chen and X. Xing, *Phys. Chem. Chem. Phys.*, 2017, **19**, 24436-24439.
44. S. Henke, A. Schneemann and R. A. Fischer, *Adv. Funct. Mater.*, 2013, **23**, 5990-5996.
45. L. D. DeVries, P. M. Barron, E. P. Hurley, C. Hu and W. Choe, *J. Am. Chem. Soc.*, 2011, **133**, 14848-14851.
46. A. D. Fortes, E. Suard and K. S. Knight, *Science*, 2011, **331**, 742-746.
47. H. Takahashi and R. Tamura, *CrystEngComm*, 2015, **17**, 8888-8896.
48. P. Lama, R. K. Das, V. J. Smith and L. J. Barbour, *Chem. Commun.*, 2014, **50**, 6464-6467.
49. H. L. Zhou, Y. B. Zhang, J. P. Zhang and X. M. Chen, *Nat. Commun.*, 2015, **6**, 6917.
50. I. Grobler, V. J. Smith, P. M. Bhatt, S. A. Herbert and L. J. Barbour, *J. Am. Chem. Soc.*, 2013, **135**, 6411-6414.
51. W. Cai and A. Katrusiak, *Nat. Commun.*, 2014, **5**, 4337.
52. H. L. Zhou, R. B. Lin, C. T. He, Y. B. Zhang, N. Feng, Q. Wang, F. Deng, J. P. Zhang and X. M. Chen, *Nat. Commun.*, 2013, **4**, 2534.
53. D. Das, T. Jacobs and L. J. Barbour, *Nat. Mater.*, 2010, **9**, 36-39.
54. R. H. Jones, K. S. Knight, W. G. Marshall, J. Clews, R. J. Darton, D. Pyatt, S. J. Coles and P. N. Horton, *CrystEngComm*, 2014, **16**, 237-243.
55. S. Bhattacharya and B. K. Saha, *CrystEngComm*, 2014, **16**, 2340.
56. M. K. Panda, T. Runčevski, S. C. Sahoo, A. A. Belik, N. K. Nath, R. E. Dinnebier and P. Naumov, *Nat. Commun.*, 2014, **5**, 4811.
57. V. G. Saraswatula and B. K. Saha, *Cryst. Growth Des.*, 2015, **15**, 593-601.
58. E. R. Engel, V. J. Smith, C. X. Bezuidenhout and L. J. Barbour, *Chem. Commun.*, 2014, **50**, 4238-4241.
59. I. de Pedro, A. García-Saiz, J. Dupont, P. Migowski, O. Vallcorba, J. Junquera, J. Rius and J. Rodríguez Fernández, *Cryst. Growth Des.*, 2015, **15**, 5207-5212.
60. B. R. Mullaney, L. Goux-Capes, D. J. Price, G. Chastanet, J. F. Létard and C. J. Kepert, *Nat. Commun.*, 2017, **8**, 1053.